

Reverse Modelling of Human Long Bones Using T-Splines - Case of Tibia

Milos STOJKOVIC, Marko VESELINOVIC, Nikola VITKOVIC, Dragan MARINKOVIC, Miroslav TRAJANOVIC,
Stojanka ARSIC, Milorad MITKOVIC

Abstract: Creating a sufficiently accurate digital model of human bone geometry for a specific patient is the starting point for personalized orthopaedic surgical treatment. Such geometrical model of a particular human bone serves as a template for designing personalized bone implant, which can be an endoprosthesis, fixator plate or even scaffold. Due to that role, the geometry of a human bone model has to be reusable and modifiable. Otherwise, design of the corresponding personalized implant for a particular human bone is a very difficult task. Modern reverse modelling techniques have greatly accelerated the creation of a bone geometric model. The prevailing modern approach is based on the use of non-uniform rational B-splines. However, recent research shows that the very complex topology of bio-shapes, such as human bones, can be reconstructed more easily using T-Splines. The presented approach of using T-splines in a modelling process allows creation of a bone model with important advantages regarding quality, flexibility and geometric accuracy. The process of reverse modelling starts from the cloud of points gained through computer-tomography images and uses selected referential geometric, i.e. anatomic entities as guiding elements in digital reconstruction of the particular bone geometry.

Keywords: CAD; human bone modelling; reverse modelling; T-splines; Tibia

1 INTRODUCTION

Stemming from the natural human desire to provide the best possible assistance to those in need for health care, biomedical engineering has evolved over the past couple of decades into an enticing research field that implements engineering knowledge and concepts to pursue this noble goal. As a highly multidisciplinary field, it spans a broad array of subfields, including: biomechanics [1], IT [2], tissue engineering [3], development of implants and exoskeleton design [4], material selection [5], simulators [6], to name but a few.

Unfortunately, many medical situations call for a bone replacement. Standard procedures require from a surgeon to shape the material to be inserted so as to fit the affected area. The geometry of the artificial material that is used to replace missing part of the natural bone should resemble the original geometry as closely as possible. Hence, the creation of accurate digital model of the original bone geometry is crucial for a successful outcome.

The very first step in creation of geometrically accurate model of the bone is to make medical digital image of the bone. Compared with X-ray and MRI (Magnetic Resonance Imaging), CT (Computer Tomography) scanning is still the medical imaging procedure with the most accurate outcome. When it comes to collecting the bone data from a healthy person, MRI is the desired method. Unlike CT and MRI, X-ray can only provide a 2D (image) scanning result. Rathnayaka [7] analysed advantages and disadvantages of both CT and MRI, and particularly emphasized those that favour CT.

The reverse modelling (RM) process starts with importing data obtained from CT and creating the cloud of points. Even if it is the most efficient approach for digital reconstruction of the bone surface, creating tessellated model is not the best option if a surgeon wants to create personalized implant from it. It is quite appropriate for visualization, but it is poor in terms of reuse and modification and that is crucial for designing the corresponding personalized implant. At least a part of geometry of the anatomically personalized implant is congruent (e.g. endoprosthesis) [8] or complementary (e.g. fixation plate) [9] to the geometry of a particular bone.

Hence, designing a personalized implant requires many interventions regarding modification of initial geometry and its reuse in geometry operations. To make the geometric model of the bone reusable and modifiable it has to be generated over the cloud of points and, at the same time, to be native to the geometric kernel of CAD (Computer-Aided Design) software. Besides its crucial role in designing of anatomically personalized implant, the patient-specific human bone geometric model may be very beneficial for orthopaedic surgery in terms of computer-based preoperative planning and surgery training simulations [10]. Bibliowicz et al. [11] highlighted advantages of a digital model over the physical one.

2 CURRENT SOLUTIONS FOR CREATING GEOMETRIC MODEL OF A HUMAN BONE

There are several methods that enable creation of a digital human bone geometric model. Generally, they can be classified into two main groups: automatic and manual methods.

2.1 Automatic Methods

In references [12, 13] a noteworthy method was presented based on reshaping (scaling) of the standard sample of the human 3D generic bone model in order to match the X-ray image of a particular patient bone. However, the model created by this method does not provide precisely defined geometric entities (points, planes, spline curves, etc.) and it can be very hard to control the accuracy of the 3D model, without a precisely defined geometry.

The most recent automatic solutions, though, which are not explicitly aimed for the digital reconstruction of human bones, but mainly for the isogeometric analysis (IGA) [14, 15] promote T-spline model, that is, T-mesh based on surface mapping and parameterization. The technology enables converting unstructured quad/hex meshes to T-spline surfaces/solids [16, 17] and it found its application for the complex topologies existing in bio-shapes. Escobar et al. [18] presented a method to construct a trivariate T-spline representation of complex genus-zero

solids, using volumetric parameterization between the solid and the parametric domain (the unitary cube in this case). An obvious disadvantage of the proposed method is the limitation to use only the genus-zero solids. For instance, a human pelvis model cannot be created by using this method. Liu et al. [19] offered a method based on arbitrary genus topology and polycube as the parametric domain for T-spline model creation. Generated models are mainly C2-continuous over the boundary surface. Li et al. [20] presented a method that generates T-spline surface model using an initially created control mesh.

The listed automatic methods are highly dependent on the quality of initial model. They usually demand a high quality of boundary or solid mesh as input data. This can be a shortcoming in real life cases when the input medical image data of a human bone gained from CT are not complete (Fig. 1), but rich of holes, noise and other errors (artifacts) and illogical, ambiguous bifurcation or trifurcation [11]. In that case, generating a valid mesh requires strenuous model pre-processing even with the help of advanced algorithms of hole filling for volumetric objects [21].

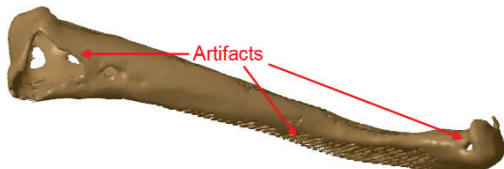


Figure 1 Polygonal model – the model of triangular mesh generated initially from the CT image input data of human clavicle

2.2 Manual (semi-automatic) Methods

Methods from this group are usually based on creation of the boundary (contour) curves from the input data, which enable further generation of the 3D bone model. Vast majority of these solutions rely on NURBS (Non-Uniform Rational B-Spline). Yoo [22] originally suggested three steps method based on B-spline interpolation. In the first step a so called base implicit surface is being created by using thin-plate radial basis functions. Later, using voxel data extracted from implicit basis surface a rectangular curve net is generated. The last step is to model B-spline surface by interpolating the rectangular array of interior points created over rectangular curve net. This method seems to be the most robust model for incomplete CT scans compared to other B-spline methods. Chougule et al. [23] tested one of the most frequently used B-spline manual method for boundary surface remodelling for metacarpus bones case. It starts with creation of B-spline contour curves through scanned points following with sweeping the surface over these series of curves. In a similar manner, but for the case of distal femur geometry (knee), Au et al. [24] proposed a NURBS-based modelling method enriched with a voxel mesh technique. Grove et al. [25], however, revealed weaknesses related to NURBS application for remodelling of bio-shapes in terms of accuracy and efficiency.

Gan et al. [26], in the search for new morphing machining strategy, proposed T-Spline to reconstruct complex shape of middle finger bone. They noticed that the application of NURBS for representation of complex shapes like bones usually requires assembling of multiple trimmed NURBS patches. The unavoidable cracks or gaps between adjacent patches violate the model integrity and,

what was crucial for manufacturing point of view, these tiny inaccuracies disable tool path generation. T-spline enables modelling of the middle finger bone shape easily by a single surface without cracks.

The gap between NURBS surfaces discussed in [15] and [27] can be overcome using a mutual B-spline as demonstrated in [28]. Therefore, the gap-free feature is not the major advantage of a T-spline surface over a NURBS surface, because both methods can provide a watertight final surface. T-spline surface is C2-continuous (curvature continuous) and with a reduced number of control points in comparison to a NURBS surface [29]. The basic problem to be resolved is to develop a three-dimensional (trivariate) representation of the solid in such a way that the surface representation is exactly preserved [15].

To explore the capabilities of T-spline surfaces application for digital reconstruction of human long bone geometry, we developed an original procedure for the case of human tibia modelling. This procedure is designed according to anatomical and morphological properties of the bones [30, 31]. Considering that the modelling procedure is applicable for NURBS as well as for T-splines, it is possible to compare these two models. At the present moment, T-Splines modelling tools are available just within Autodesk Fusion 360 and within last Plug-Ins for Rhinoceros and SolidWorks.

3 INPUT DATA

As it was described herein before, reverse modelling of a human bone's geometry using CAD software implies generating digital 3D surface or solid model of the bone's geometry from the image data generated by a radiology imaging device (X-Ray, CT, MRI). In this case, CT scans of human tibia of Caucasian adult made by 64-slice CT (MSCT, Aquillion 64, Toshiba) in the resolution of 0.5 mm, are used as raw data.

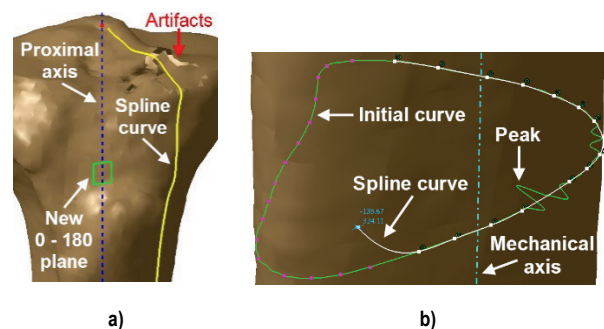


Figure 2 Initial polygonal model, a) Created spline at proximal tibia, b) Spline creation at tibia shaft

The CT data are being transformed into a cloud of points over which initial polygonal, that is, tessellated model is being created (Fig. 2). In the next phase of reverse modelling, the geometrical elements that are native to kernel of CAD software (points, planes, lines and curves) are being designed as presented in [8]. CATIA V5 R19 CAD software was used for these first two stages.

4 APPLIED MODELLING PROCEDURE

Situated at the medial side of the leg, tibia, except for the femur, is the longest bone of the skeleton. It has a body and two ends, proximal (upper) and distal (lower). The proximal

end of the tibia has a broad superior articular surface which articulates with the femur. The body or shaft has prismoid shape with three surfaces and three margins. The anterior margin, the most prominent of the three, commences above at the tuberosity, and ends below at the anterior margin of the medial malleolus. The distal end of the tibia, much smaller than the upper, is prolonged downwards on its medial side as a strong process, the medial malleolus. Its inferior articular surface is quadrilateral and smooth for articulation with the talus [32].

4.1 Creation of Referential Geometric Entities

This stage of reverse modelling of human tibia geometric model is based on the procedure that is described in [28], [33]. It leads towards an initial NURBS model that will be used as a base model for further improvement by T-splines and for comparison. In the case of tibia, the mechanical axis is a line from the centre of the tibia plateau (interspinous intercruciate midpoint) extending distally to the centre of the tibia plafond [34] (Fig. 3-a). The tibia plateau (proximal articular surface) is approximated with ellipse and the first point that defines mechanical axis is centre of the ellipse, which is approximately equal to centre of tibia spines notch [34]. The centre of the tibia plafond (distal articular surface) is approximated with gravity centre of tibia plafond cross-sections at the distal end of tibia.

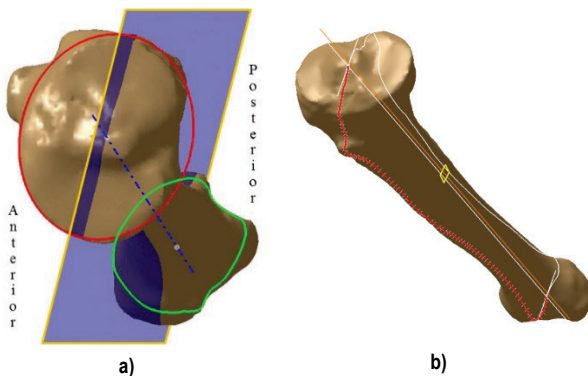


Figure 3 Determination of points defining the mechanical axis

Once the mechanical axis is determined, it is possible to position variously oriented planes which are in accordance with the anatomy of tibia. Lateral-Medial (L-M) plane contains the mechanical axis of tibia and divides it into lateral and medial sides (Fig. 3-b).

The initial contour curves for the distal part are obtained at the intersection of the initial polygonal model and the half-planes that pass through mechanical axis and are oriented at: 0, 10, 20, 30, 40, 50, 60, 70, 80, 90, 105, 120, 135, 150, 165, 180, 195, 210, 225, 240, 255, 270, 285, 300, 310, 325, 335 and 345 degrees in direction from the lateral to anterior side. Thus, the A-P plane determines the contour curves of distal tibia region at 0 and 180 degrees (Fig. 4-a).

The initial contour curves for tibia's body region are created using series of planes perpendicular to the mechanical axis of tibia (Fig. 4-b).

In the case of contour curves for proximal part, rotating the half-planes around mechanical axis of tibia leads to irregular curves distribution at transition from the proximal

part to the tibia shaft, because the mechanical axis is much closer to the posterior side than the anterior side in that region. For this reason, a "local mechanical axis" relevant to the proximal part is created, connecting the centre of the tibia plateau with the lowest cross-section of the proximal part, which is perpendicular to the mechanical axis of tibia. This local axis is used as referential, and the half-planes that pass through it are oriented at: 0, 15, 30, 46, 60, 75, 85, 93, 105, 115, 125, 135, 145, 155, 165, 180, 195, 210, 225, 240, 255, 270, 285, 295, 305, 315, 330 and 345 degrees. This is similar to the scenario of creation of initial contour curves for distal part, only with the new "local" axis as referential (Fig. 4-a).

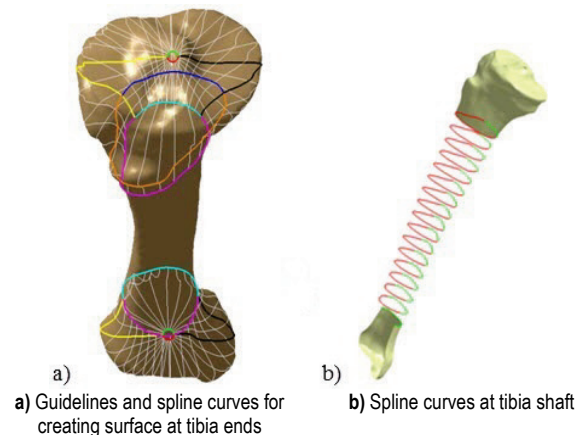


Figure 4 The initial contour curves of tibia segments

All these initial contour curves (from all three parts of the tibia) are used for positioning the points which, when connected, create the spline curves (Fig. 2-a, 2-b). Usually, the initial curves are characterized with sporadic peaks, which do not represent the real geometry of the bone boundary surface but originate from interpolating over the points of poor and incomplete initial polygonal model. Due to this issue, the initial curves have to be replaced with spline curves (Fig. 2-b), which can approximate the parts of the initial model that contain holes and other artefacts (Fig. 2-a). Moreover, the spline curves enable further creation of boundary surfaces of particular tibia. The solid model, if there is a need for it, can be obtained by filling the volume of the surface model. All planes and half-planes are placed so that the created curves describe this specific tibia in anatomically correct way and having in mind further T-spline surface creation.

4.2 Creation of T-spline Surface Improving Initial NURBS Model

Once created, the spline curves are imported into CAD software that embraces T-Spline modelling tools (for this study we have used T-splines plug-in for Rhinoceros). All curves are then rebuilt from polynomial degree 5 to degree 3, which is the recommended standard in CAD [35]. In addition, curves in junction areas of tibia regions (distal to shaft, shaft to proximal) are rebuilt to the same number of control points (CP): 40 for the distal curves, and 70 for proximal curves and 28 for the set of shaft curves. For the distal and proximal curves, the number of CPs is further reduced compared to the mean number of CPs that curves had after the initial import into CAD software. An

additional constraint, which allowed this control points reduction was the threshold regarding maximal deviation between the new and old curve that is measured from the control points. In particular, the threshold for the distal curves was 0.05 mm and 0.16 mm for the proximal curves. These adjustments are recommended to generate uniform T-spline surfaces for the distal and proximal parts efficiently, keeping relatively simple geometry (Fig. 5-a and 5-b). A simple geometry is easier to manipulate and consumes less memory.

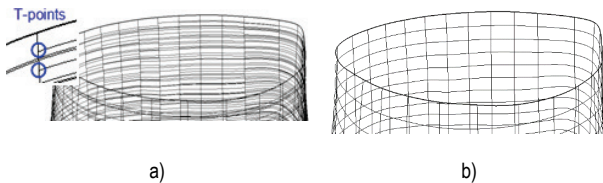


Figure 5 T-spline surface (mesh) of distal tibia region at junction area with tibia shaft boundary surface, a) Before adjustments of control points there are too many T-points in the mesh and surface is unnecessarily complex; b) After the adjustments, mesh is without T-points

To connect the geometries of all three components of the tibia's boundary surface with minimal folds and wraps, curves which will shape the tibia shaft boundary surface should be controlled by 28 control points because there are altogether 28 distal and 28 proximal curves. This adjustment causes the maximal deviation of 0.24 mm between new and old shaft curves. The adapted spline curves of all three tibia's regions are presented in Fig. 6.

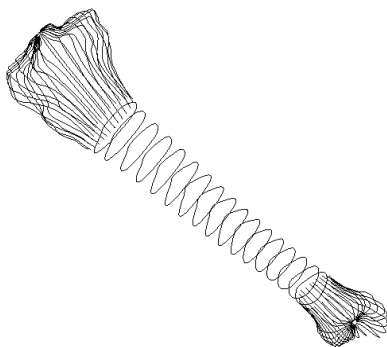


Figure 6 Three sets of adapted curves of corresponding tibia's regions

The next step in creating of T-spline surface is done by using T-splines modelling tools given in the CAD software plug-in. Three separated T-spline surfaces (i.e. segments) that correspond to three different tibia's anatomical regions are created by applying the Loft tool on the adequate set of curves. These three segments are then connected into one with the Bridge tool, and this is exactly where the importance of the proximal curves created with the "local" axis and the shaft curves with 28 control points come to the fore. Namely, the connection surface made by Bridge tool can be applied between the two boundary edges of different surfaces with the same number of control points (28 in this case). To evade the unnatural wrapping of connection surface showed in Fig. 7-a, the control points' positions on the two boundary edges of two different surfaces that are connecting should coincide as much as it is possible. Usage of the "local" axis in creation of proximal curves makes these curves evenly positioned, so the end-points of these curves, which become the control points of the boundary

edge of proximal T-spline segment, coincide better with the control points of boundary edge of shaft segment. (Fig. 7-b and 7-c)

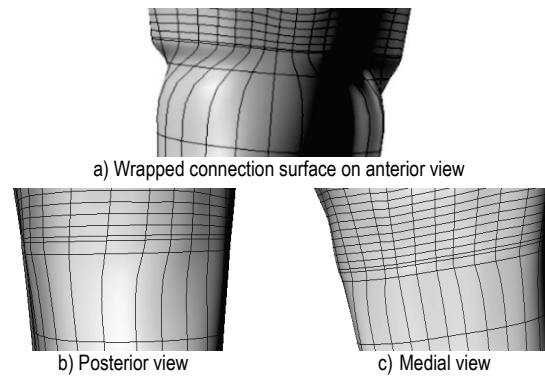


Figure 7 Coinciding the control points of boundary edges of two surfaces improves the geometrical accuracy of the connection surface making it more natural

Small surface irregularity like a wrinkle at the distal and proximal ends, near the apexes, i.e. the points defining the mechanical axis of tibia, shown in Fig. 8-a, can be corrected by deleting excess edges, and this is possible due to the row termination by the T-point (Fig. 8-b). These irregularities appear because of applying rotational sweep CAD feature to create a surface over the close and choppy curves in this area.

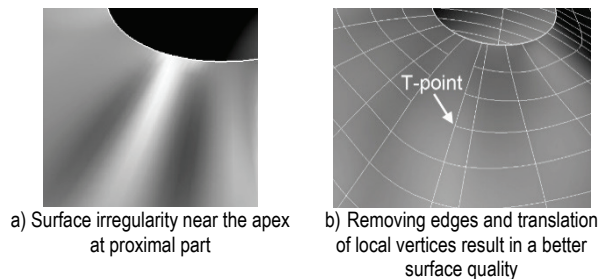


Figure 8 Local refining of T-spline surface

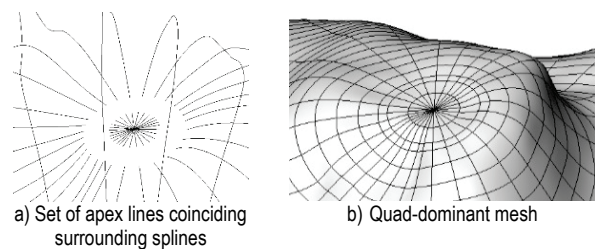


Figure 9 First solution for the remaining hole at tibia plateau

The last step in this phase is mending two small holes of 2.5 mm radius on the proximal and distal apices. Creating of these holes in both apices is inevitable because the spline curves in both sets, distal and proximal, do not have a common intersection point. There are two basic solutions to approximately generate these surfaces. The first one is to create a set of very short new 28 lines through the apex (Fig. 9-a), rebuild them as it was previously described, create a circumferential flat surface using Loft tool, and then connect it with the previously created T-spline surface using Bridge tool (Fig. 9-b).

The second scenario is to use the Fill hole tool (Fig. 10), which is much simpler than the first method.

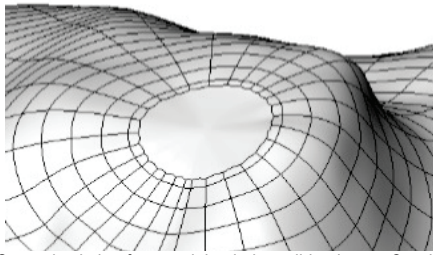


Figure 10 Second solution for remaining hole at tibia plateau Quad mesh

Due to the small size of the hole, there is no significant difference in the surface accuracy between the two methods, but the mesh structure is important for prospective analyses. Namely, the first method gives a quad-dominant mesh (quads - four sided polygons), with a few triangles. Mesh created with the second method consists only of quads (completely-quad).

5 RESULTS: IMPROVEMENTS REGARDING INITIAL NURBS MODEL

The created T-spline based model shown in Fig. 11 is a T-mesh consisting of three segments: proximal (upper) end, shaft (body) and distal (lower) end, which are smoothly connected into one surface.

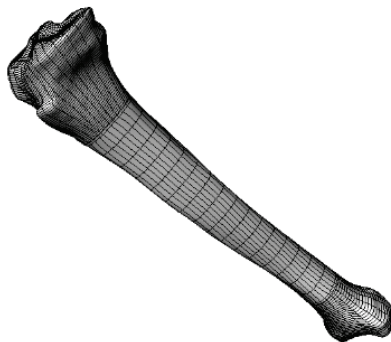


Figure 11 Single T-spline surface (mesh) - shaded model

5.1 Surface Continuity

Created using the presented method, T-mesh becomes a single surface entirely C2-continuous, which has been proven with the Zebra analysis [36] shown in Fig. 12.

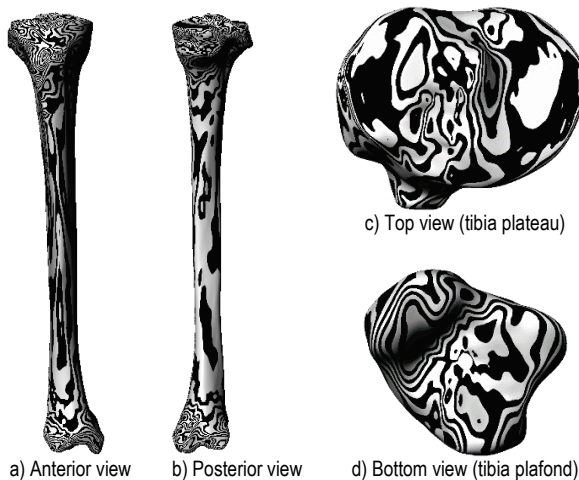


Figure 12 Zebra analysis of T-splines surface

Besides other benefits coming from enhanced surface continuity, this feature is very significant from the manufacturing point of view, because it enables creating the smooth (unbroken) toolpaths [26].

For comparison, a corresponding NURBS-based model of the same bone was designed [28]. The NURBS surface segments were created in the same manner as the T-spline surface segments. In addition, very similar or the same CAD tools were used to create the surface transition blends and holes' patches. Yet, the NURBS-based model of the same bone cannot be united in a single C2-continuous surface, but it stays an assembly of several surface segments as presented in [28, 33]. Due to these connections between the surface segments, the surface continuity is only C0 along the segment borders (Fig. 13).



Figure 13 Zebra analysis of NURBS surface clearly shows discontinuity of reflection stripes at the border between adjacent shaft and distal surface segment

5.2 Geometric Accuracy

To determine the deviations in geometry regarding initial polygonal model, both the T-spline based model and NURBS based model are compared with the initial surface model in Catia software (Fig. 14).

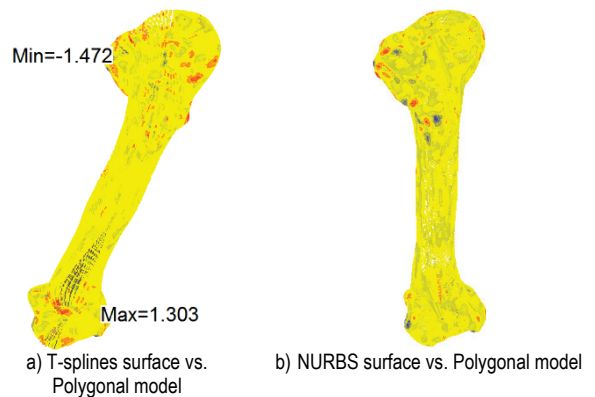


Figure 14 Deviation analysis

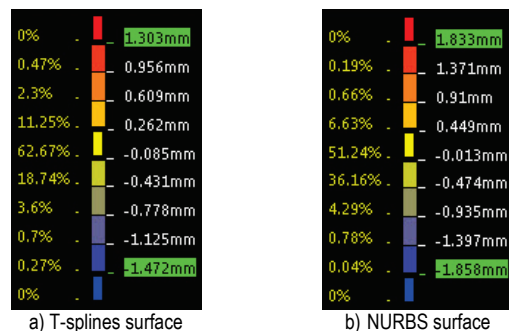


Figure 15 Results of "point to point" deviation analyses

The numeric results of comparison are presented in Fig. 15. The scales indicate how much of the surface of these two models deviates from the surface of the initial, polygonal model and to what extent (e.g. 8.74% of the T-spline based model deviates -0.431 mm, while 36.16% of the NURBS based model deviates -0.474 mm from the polygonal model).

The greatest deviations appear at the proximal and distal ends. This is expected as these regions are geometrically most complex. However, in both cases (T-splines and NURBS), vast majority of points deviate less than 1 mm, which is negligible from the perspective of surgical operation and even from the perspective of design and manufacturing of custom-to-patient implants (endoprotheses, fixating plates and scaffolds). Fig. 16 visualizes the deviation in terms of numbers.

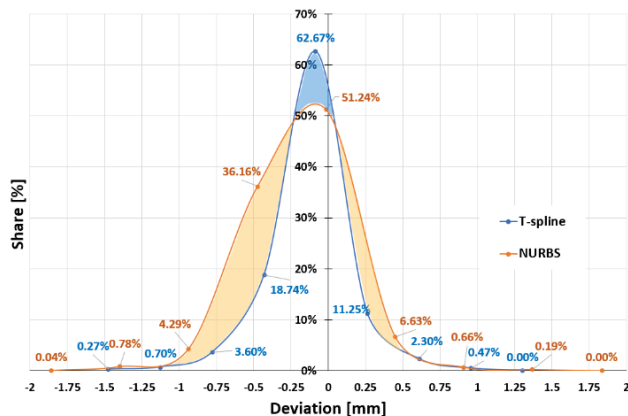


Figure 16 Share and extent of deviation between T-spline and NURBS surface and polygonal model's surface, respectively (data from "point to point" deviation analyses)

5.3 Geometric Flexibility

Another important advantage of geometric models based on T-splines in comparison with those based on NURBS is the ability to act like a digital clay model. Thanks to the T-points, it is possible to add an edge in the T-splines surface (mesh) locally or to subdivide a face in the surface in order to have more control over the surface at some places (refinement). The T-splines surface stays watertight and C^2 -continuous, and with a less number of control points in comparison with a similar NURBS surface [29]. This great flexibility along with the high surface quality and sufficient geometric accuracy make the T-spline based models ideal for custom-to-patient implant development.

6 DISCUSSION

Having in mind all the advantages of using T-splines in digital reconstruction of human bone geometry, which have been highlighted hereinbefore, the future challenge is to parametrize the T-mesh for a specific complex shape, which is characterized by the numerous variants of the same topology. In this way the formed T-mesh may be applied as a kind of generic geometric model for a specific bone, like human tibia or just a region of a human bone (e.g. tibia plateau, which is directly related to the geometry of personalized knee implant). By changing a few parameters that correspond to specific anatomical and

morphometric measurements, captured from X-ray or CT images by orthopaedic surgeon, it is possible to change polyhedron of control points and enable efficient control of the T-mesh shape, keeping sufficient geometric accuracy and quality of the reconstructed surface. In this way it will be possible to automate the design of the personalized bone implant. The pre-condition for this scenario is to define an optimal polyhedron of control points, which will engage the minimal needed number of control points harnessed by proper mutual relations and morphometric parameters, creating a manageable T-mesh that can take a shape of numerous variants of the same topology.

7 CONCLUSION

This paper considered the application of T-splines in geometric modelling of objects characterized by complex topology such as bones, demonstrating the advantages offered by this approach.

The basic principles in the presented method for digital reconstruction of tibia geometry can be used for creation of geometric models of any human long bone. One of the most important achievements of the applied method is that the created T-spline model of tibia is built according to anatomical features and its shape can be driven by the set of prominent morphometric parameters of the specific bone. This defines the basis for parametrization of the T-mesh in future.

The T-spline surface created for the case of human tibia is characterized by high quality reflected in C^2 surface continuity and great congruency with the initial polygonal model of the bone. In addition, it has clear advantages in comparison with the surface created with NURBS, especially regarding surface quality, geometric flexibility and local refinement.

In certain cases, the generation of bone geometric models may be the final objective, for instance when a bone replacement (endoprotheses or scaffold) is to be manufactured. But in many cases, this is only a necessary step in performing a further structural analysis. Although this aspect is not in the focus of this paper, it is obvious that the properties of the developed model favour a later FE analysis, particularly the isogeometric analysis. This is primarily due to the C^2 -continuity and the quad-dominated or even quad-only surface representation.

In the future, the biggest challenge regarding using T-splines in digital reconstruction of the bones geometry is likely to be its full and robust parametrization, i.e. enabling a T-spline mesh to easily take the shape of a patient specific bone (e.g. tibia or mandible). In other words, the generic T-spline mesh built for a specific bone should be controlled by just a few parameters that directly correlate to distinctive morphometric measurements that the surgeon can capture while examining radiologic image.

Acknowledgements

This paper reports on a part of research within the project III41017 - Virtual human osteoarticular system and its application in preclinical and clinical practice, funded by the Ministry of Education, Science and Technological Development of the Republic of Serbia, for the period of 2011-2018.

8 REFERENCES

- [1] Guilak, F., Butler, D. L., Goldstein, S. A., & Baaijens, F. P. T. (2014). Biomechanics and mechanobiology in functional tissue engineering. *Journal of Biomechanics*, 47(9), 1933-1940. <https://doi.org/10.1016/j.jbiomech.2014.04.019>
- [2] Mišić, D., Manić, M., Vitković, N., & Korunović, N. (2015). Toward an Integrated Information System for the Design, Manufacturing and Application of Customized Implants. *Facta Universitatis-Series Mechanical Engineering*, 13(3), 307-323.
- [3] Balint, R., Cassidy, N. J., & Cartmell, S. H. (2014). Conductive polymers: Towards a smart biomaterial for tissue engineering. *Acta biomaterialia*, 10(6), 2341-2353. <https://doi.org/10.1016/j.actbio.2014.02.015>
- [4] Poliakov, A., Pakhaliuk, V., Lozinskiy, N., Kolesova, M., Bugayov, P., & Shtanko P. (2016). Biosimilar Artificial Knee for Transfemoral Prostheses and Exoskeletons. *Facta Universitatis-Series Mechanical Engineering*, 14(3), 321-328. <https://doi.org/10.22190/FUME1603321P>
- [5] Ristić, M., Manić, M., Mišić, D., Kosanović, M., & Mitković, M. (2017). Implant Material Selection Using Expert System. *Facta Universitatis-Series Mechanical Engineering*, 15(1), 133-144. <https://doi.org/10.22190/FUME160723004R>
- [6] Marinkovic, D. & Zehn, M. (2018). Corotational finite element formulation for virtual-reality based surgery simulators. *Physical Mesomechanics*, 21(1), 15-23. <https://doi.org/10.1134/S1029959918010034>
- [7] Rathnayaka, K. (2011). 3D Reconstruction of Long Bones Utilising Magnetic Resonance Imaging (MRI). (*Doctoral dissertation*), Retrieved from https://eprints.qut.edu.au/49779/1/Kanchana_Rathnayaka_Mudiyanselage_Thesis.pdf
- [8] Stojkovic, M. S., Milovanovic, J. D., Vitković, N. M., Trajanović, M. D., Grujovic, N., Milojevic, V., Milisavljevic, S., & Mrvic, S. (2010). Reverse modeling and solid free-form fabrication of sternum implant. *Australasian Physical & Engineering Sciences in Medicine*, 33(3), 243-250. <https://doi.org/10.1007/s13246-010-0029-1>
- [9] Stevanović, D. M., Vitković, N. M., Veselinović, M. M., Trajanović, M. D., Manić, M. T., & Mitković, M. B. (2013). Parametrization of Internal Fixator by Mitkovic. In Majstorović V. D., (Ed.), *The 7th International Working Conference TQM - Advanced and Intelligent Approaches*, Belgrade, 3-7 June, 541-544.
- [10] Sourina, O., Sourin, A., & Sen, H. T. (2007). Orthopedic Surgery Training Simulation. *Journal of Mechanics in Medicine and Biology*, 7(1), 37-53. <https://doi.org/10.1142/S0219519407002121>
- [11] Bibliowicz, J., Khan, A., Agur, A., & Singh, K. (2011). High-Precision Surface Reconstruction of Human Bones from Point-Sampled Data. *ISHS 2011 Conference Proceedings: International Summit on Human Simulation*, 1-10.
- [12] Filippi, S., Motyl, B., & Bandera, C. (2008). Analysis of existing methods for 3D modelling of femurs starting from two orthogonal images and development of a script for a commercial software package. *Computer methods and programs in biomedicine*, 89(1), 76-82. <https://doi.org/10.1016/j.cmpb.2007.10.011>
- [13] Gunay, M., Shim, M. B., & Shimada, K. (2007). Cost- and time-effective three-dimensional bone-shape reconstruction from X-ray images. *The international journal of medical robotics and computer assisted surgery*, 3, 323-335. <https://doi.org/10.1002/rcs.162>
- [14] Scott, M. A., Simpson, R. N., Evans, J. A., Lipton, S., Bordas, S. P. A., Hughes, T. J. R., & Sederberg, T. W. (2013). Isogeometric boundary element analysis using unstructured T-splines. *Computer Methods in Applied Mechanics and Engineering*, 254, 197-221. <https://doi.org/10.1016/j.cma.2012.11.001>
- [15] Evans, E. J., Scott, M. A., Li, X., Thomas, D. C. (2015). Hierarchical T-splines: Analysis-suitability, Bézier extraction, and application as an adaptive basis for isogeometric analysis. *Computer Methods in Applied Mechanics and Engineering*, 284, 1-20. <https://doi.org/10.1016/j.cma.2014.05.019>
- [16] Zhang, Y. J., (Ed.). (2013). *Image-Based Geometric Modeling and Mesh Generation, Series: Lecture Notes in Computational Vision and Biomechanics*, 3, Springer. <https://doi.org/10.1007/978-94-007-4255-0>
- [17] Wang, W., Zhang, Y., Scott, M. A., & Hughes, T. J. R. (2011). Converting an unstructured quadrilateral mesh to a standard T-Spline surface. *Computational Mechanics*, 48(4), 477-498. <https://doi.org/10.1007/s00466-011-0598-1>
- [18] Escobar, J. M., Cascón, J. M., Rodríguez, E., & Montenegro, R. (2011). A new approach to solid modeling with trivariate T-splines based on mesh optimization. *Computer Methods in Applied Mechanics and Engineering*, 200, 3210-3222. <https://doi.org/10.1016/j.cma.2011.07.004>
- [19] Liu, L., Zhang, Y., & Wang, W. (2015). Feature-Preserving T-mesh Construction Using Skeleton-based Polycubes. *Computer Aided Design*, 58, 162-172. <https://doi.org/10.1016/j.cad.2014.08.020>
- [20] Li, W.-C., Ray, N., & Lévy, B. (2006). Automatic and Interactive Mesh to T-Spline Conversion. Polthier, K., Sheffer, A., (Eds.): *Eurographics Symposium on Geometry Processing*, p. 10, retrieved from http://alice.loria.fr/publications/papers/2006/SGP_Splines/SGP06-fin-electronic_mesh_to_spline.pdf
- [21] Janaszewski M., Couprie M., & Babout L. (2010). Hole filling in 3D volumetric objects. *Pattern Recognition*, 43(10) 3548-3559. <https://doi.org/10.1016/j.patcog.2010.04.015>
- [22] Yoo, D. J. (2011). Three-dimensional surface reconstruction of human bone using a B-spline based interpolation approach. *Computer-Aided Design*, 43(8), 934-947. <https://doi.org/10.1016/j.cad.2011.03.002>
- [23] Chougule, V. N., Mulay, A. V., & Ahuja, B. B. (2016). Methodologies for Development of Patient Specific Bone Models from Human Body CT Scans. *J. Inst. Eng. India Ser. C*. 1-6. <https://doi.org/10.1007/s40032-016-0301-6>
- [24] Au, A. G., Palathinkal, D., Liggins, A. B., Raso, J. V., Carey, J., Lambert, R. G., & Amirfazli, A. (2008). A NURBS-based technique for subject-specific construction of knee bone geometry. *Computer Methods and Programs in Biomedicine*, 92(1), 20-34. <https://doi.org/10.1016/j.cmpb.2008.05.009>
- [25] Grove, O., Rajab, K., Piegl, L. A., & Lai-Yuen, S. (2011). From CT to NURBS: Contour Fitting with B-spline Curves. *Computer-Aided Design and Applications*, 8(1), 3-21. <https://doi.org/10.3722/cadaps.2011.3-21>
- [26] Gan, W. F., Fu, J. Z., Shen, H. Y., & Lin, Z. W. (2014). A morphing machining strategy for artificial bone. *Journal of Zhejiang University SCIENCE A*, 15(3), 157-171. <https://doi.org/10.1631/jzus.A1300274>
- [27] Sederberg, T. W., Zheng, J., Bakenov, A., & Nasri, A. (2003). T-splines and T-NURCCS. *ACM Transactions on Graphics*, 22(3), 477-484. <https://doi.org/10.1145/882262.882295>
- [28] Veselinovic, M. Vitković, N., Trajanović, M., Stevanović, D., Manić, M., Arsić, S., & Petrović, S. (2013). Different Approaches for Creation of Human Tibia 3D Models Based on CT Data. *The 35th International Conference on Production Engineering*, Kraljevo-Kopaonik, 283-289.
- [29] Sederberg, T. W., Cardon, D. C., Finnigan, G. T., North, N. N., Zheng, J., & Lyche, T. (2004). T-splines Simplification and Local Refinement. *ACM Transactions on Graphics*, 23(3), 276-283. <https://doi.org/10.1145/1015706.1015715>
- [30] Vitković, N., Milovanović, J., Korunović, N., Trajanović, M., Stojković, M., Mišić, D., & Arsić, S. (2013). Software

- system for creation of human femur customized polygonal models. *Computer Science and Information Systems*, 10(3), 1473-1497. <https://doi.org/10.2298/CSIS121004058V>
- [31] Majstorovic, V., Trajanovic, M., Vitkovic, N., & Stojkovic, M. (2013). Reverse engineering of human bones by using method of anatomical features. *CIRP Annals – Manufacturing Technology*, 62(1), 167-170. <https://doi.org/10.1016/j.cirp.2013.03.081>
- [32] Moore, K., Dalley, A., & Agur, A. (2010). Lower Limb / Tibia, Taylor, C., Heise, J., Montalbano, J. (Eds.), *Clinically Oriented Anatomy*, Philadelphia, USA: Lippincott Williams & Wilkins, 520-521.
- [33] Veselinovic, M. Vitković, N., Stevanović, D., Trajanović, M., Arsić, S., Milovanović, J., & Stojković, M. (2011). Study on creating human tibia geometrical models. Costin, H. Morega, Al., Vereștiuc, L. (Eds.): *Proceedings of the 3rd International Conference on E-Health and Bioengineering - EHB*, Iași, Romania, 24-26 November, 195-198.
- [34] Cooke, D., Sled, E., & Scudamore, A. (2007). Editorial, Frontal Plane Knee Alignment: A Call for Standardized Measurement. *The Journal of Rheumatology*, 34(9), 1796-1801
- [35] Cheng, R. K. C. (2014). *Inside Rhinoceros 5*. Stamford, CT, USA: Cengage Learning.
- [36] Hahmann, S. (1999). *Visualization techniques for surface analysis*, In C. Bajaj (ed.): *Advanced Visualization Techniques*, John Wiley, retrieved from <http://ljk.imag.fr/membres/Stefanie.Hahmann/PUBLICATIONS/H99.pdf>

Contact information:

Milos STOJKOVIC, PhD Assistant Professor
(Corresponding author)
University of Nis, Faculty of Mechanical Engineering,
Aleksandra Medvedeva 14, 18000, Nis, Serbia
milos.stojkovic@masfak.ni.ac.rs

Marko VESELINOVIC, PhD candidate
University of Nis, Faculty of Mechanical Engineering,
Aleksandra Medvedeva 14, 18000, Nis, Serbia
veselinovic.marko.meng@gmail.com

Nikola VITKOVIC, PhD Assistant Professor
University of Nis, Faculty of Mechanical Engineering,
Aleksandra Medvedeva 14, 18000, Nis, Serbia
nikola.vitkovic@masfak.ni.ac.rs

Dragan MARINKOVIC, PhD Associate Professor
Department of Structural Analysis, Berlin Institute of Technology,
Str. d. 17. Juni 135, 10623 Berlin, Germany
dragan.marinkovic@tu-berlin.de

Miroslav TRAJANOVIC, PhD Professor
University of Nis, Faculty of Mechanical Engineering
Aleksandra Medvedeva 14, 18000, Nis, Serbia
miroslav.trajanovic@masfak.ni.ac.rs

Stojanka ARSIC, PhD Associate Professor
University of Nis, Faculty of Medicine,
Blvd. Dr Zorana Djindjica 81, 18000 Nis, Serbia
stojanka@medfak.ni.ac.rs

Milorad MITKOVIC, PhD Professor
University of Nis, Faculty of Medicine,
Blvd. Dr Zorana Djindjica 81, 18000 Nis, Serbia
mitkovic@gmail.com